

Higgs and Z-boson production with a jet veto

Andrea Banfi,¹ Pier Francesco Monni,² Gavin P. Salam,^{3,4,5} Giulia Zanderighi⁶

¹ *Albert-Ludwigs-Universität Freiburg, Physikalisches Institut, D-79104 Freiburg, Germany*

² *Institut für Theoretische Physik, Universität Zürich, CH-8057 Zürich, Switzerland*

³ *CERN, PH-TH, CH-1211 Geneva 23, Switzerland*

⁴ *Department of Physics, Princeton University, Princeton, NJ 08544, USA*

⁵ *LPTHE; CNRS UMR 7589; UPMC Univ. Paris 6; Paris, France*

⁶ *Rudolf Peierls Centre for Theoretical Physics, 1 Keble Road, University of Oxford, UK*

We derive first next-to-next-to-leading logarithmic resummations for jet-veto efficiencies in Higgs and Z-boson production at hadron colliders. Matching with next-to-next-to-leading order results allows us to provide a range of phenomenological predictions for the LHC, including cross-section results, detailed uncertainty estimates and comparisons to current widely-used tools.

In searches for new physics at hadron colliders such as the Tevatron and CERN's Large Hadron Collider (LHC), in order to select signal events and reduce backgrounds, events are often classified according to the number of hadronic jets — collimated bunches of energetic hadrons — in the final state. A classic example is that of the search for Higgs production via gluon fusion with a subsequent decay to W^+W^- [1, 2]. A potentially severe background comes from $t\bar{t}$ production, whose decay products also include a W^+W^- pair. However, this background can be separated from the signal because its W^+W^- pair usually comes together with hard jets, since in each top decay the W is accompanied by an energetic (b) quark.

Relative to classifications based on objects such as leptons (used e.g. to identify the W decays), one of the difficulties of using hadronic jets is that they may originate not just from the decay of a heavy particle, but also as Quantum Chromodynamic (QCD) radiation. This is the case in our above example, where the incoming gluons that fuse to produce a Higgs boson will quite often radiate additional partons. Consequently, vetoing the presence of jets will eliminate much of the $t\bar{t}$ background, but it will also remove some fraction of signal events. For a full interpretation of the search results, including measurements of Higgs properties, it is crucial to be able to determine precisely what fraction of the signal survives the jet veto, which depends for example on the transverse momentum threshold $p_{t,\text{veto}}$ used to identify vetoed jets. A similar need arises in the context of the use of jet vetoes in a number of other cases involving the production of colourless heavy particles.

One way to evaluate jet-veto efficiencies is to use a fixed order perturbative expansion in the strong coupling α_s , for example as in the next-next-to-leading order (NNLO) calculations of Higgs-boson production of [3, 4]. Such calculations however become unreliable when $p_{t,\text{veto}}$ becomes too small, since large terms $\alpha_s^n L^{2n}$, with $L = \ln(M/p_{t,\text{veto}})$ and M the boson mass, appear in the cross-section to all orders in the coupling constant. These enhanced classes of terms can, however, be resummed to all orders in the coupling, often involving a functional form $\exp(Lg_1(\alpha_s L) + g_2(\alpha_s L) + \alpha_s/\pi g_3(\alpha_s L) + \dots)$.

There exist next-to-next-to-leading logarithmic

(NNLL) resummations, involving the $g_n(\alpha_s L)$ functions up to and including g_3 , for a number of quantities that are more inclusive than a jet veto: e.g. a Higgs or vector-boson transverse momentum [5–8], the beam thrust [9], and related observables [10, 11]. To obtain estimates for jet vetoes, some of these calculations have been used to reweight [9, 12, 13] parton-shower predictions [14, 15] matched to NLO results [16, 17]. However, with such a reweighting, the NNLO and/or NNLL accuracy of the original calculation does not carry through to the jet veto prediction.

Recently there has been progress towards a direct NNLL calculation of the jet veto efficiency. Full NLL results and some of the NNLL ingredients for Higgs and vector-boson were provided in [18]. Ref. [19] has used these and other ingredients to attempt to obtain a NNLL calculation for the Higgs-boson case. In this letter we show how to use the results of [18] together with those from boson p_t resummations [5–8] to obtain full NNLL accuracy. We will also examine the phenomenological impact of our results, including a matching to the NNLO predictions. Given the ubiquity of jet cuts in hadron-collider analyses, the understanding gained from our analysis has a potentially wide range of applications.

The core of boson transverse-momentum (p_t^B) resummations lies in the fact that soft and collinear emissions at disparate rapidities are effectively emitted independently. Summing over an arbitrary number of independent emissions one obtains the differential cross section for the boson as

$$\frac{d\Sigma^{(B)}}{d^2 p_t^B} = \sigma_0 \int \frac{d^2 b}{4\pi^2} e^{-ib \cdot p_t^B} \sum_n \frac{1}{n!} \prod_{i=1}^n \int [dk_i] M^2(k_i) (e^{ib \cdot k_{ti}} - 1), \quad (1)$$

where σ_0 is the leading-order total cross section, $[dk_i] M^2(k_i)$ is the phase-space and matrix-element for emitting a soft and collinear gluon of momentum k_i , while the exponential factors and integral over b encode in a factorised form the constraint relating the boson transverse momentum and those of the individual emissions $\delta^2(p_t^B - \sum_{i=1}^n k_{ti})$ [20]. The -1 term in the round brackets arises because, by unitarity, virtual corrections come with a weight opposite to that of real emissions, but don't

contribute to the p_t^B sum.

To relate Eq. (1) to a cross section with a jet-veto, let us first make two simplifying assumptions: that the independent-emission picture is exact and that a jet algorithm clusters each emission into a separate jet. The re-summation for the cross section for the highest jet transverse momentum to be below some threshold p_t^J , considering jets at all rapidities, is then equivalent to requiring all emissions to be below that threshold:

$$\begin{aligned}\Sigma^{(J)}(p_t^J) &= \sigma_0 \sum_{n=0}^{\infty} \frac{1}{n!} \prod_{i=1}^n \int [dk_i] M^2(k_i) (\Theta(p_t^J - k_{ti}) - 1) \\ &= \sigma_0 \exp \left[- \int [dk_i] M^2(k_i) \Theta(k_{ti} - p_t^J) \right],\end{aligned}\quad (2)$$

with the same universal matrix element $M^2(k_i)$ entering Eqs. (1) and (2).

Eq. (2) is clearly an oversimplification. Firstly, even within the independent emission picture, two emissions that are close in rapidity y and azimuth ϕ can be clustered together into a single jet. Let us introduce a function $J(k_1, k_2)$ that is 1 if k_1 and k_2 are clustered together and 0 otherwise. If we concentrate on the 2-emission contribution to Eq. (2), it is straightforward to see that clustering leads to a correction given by the difference between the veto with and without clustering:

$$\begin{aligned}\mathcal{F}^{\text{clust}} \sigma_0 &= \frac{\sigma_0}{2!} \int [dk_1][dk_2] M^2(k_1) M^2(k_2) \times J(k_1, k_2) \\ &\quad (\Theta(p_t^J - k_{t,12}) - \Theta(p_t^J - k_{1,t})\Theta(p_t^J - k_{2,t})).\end{aligned}\quad (3)$$

where $k_{12} = k_1 + k_2$ (throughout, we assume the standard E -scheme recombination procedure, which simply adds 4-vectors). This contribution has a logarithmic structure $\alpha_s^2 L$, i.e. NNLL, with each emission leading to a power of α_s , while the L factor comes from the integral over the rapidities allowed for the emissions ($|y| \lesssim \ln(M/p_{t,\text{veto}})$).

Considering cases with more than two emissions, two situations are possible: (1) three or more emissions may be close in rapidity, giving extra powers of α_s without extra log-enhancements (i.e. $N^3\text{LL}$ and beyond); (2) any number of emissions may be far in rapidity, each one giving an extra factor $\alpha_s L$, i.e. also NNLL. The latter contribution is however very simple because, independently of whether the two nearby emissions clustered, those that are far away must still have $p_{ti} < p_{t,\text{veto}}$. Thus the full “clustering” correction to the independent-emission picture is a multiplicative factor $(1 + \mathcal{F}^{\text{clust}})$, as first derived in detail in the appendix of [18] using results from [21].

For the generalised- k_t family of jet algorithms [22–26], with a jet radius parameter R , the function J is given by $J(k_1, k_2) = \Theta(R^2 - (y_1 - y_2)^2 - (\phi_1 - \phi_2)^2)$ and at NNLL accuracy, Eq. (3) evaluates to [18] $\mathcal{F}^{\text{clust}} = 4\alpha_s^2(p_{t,\text{veto}})CLf^{\text{clust}}(R)/\pi^2$ with

$$f^{\text{clust}}(R) = \left(-\frac{\pi^2 R^2}{12} + \frac{R^4}{16} \right) C, \quad (4)$$

for $R < \pi$, where C is $C_F = \frac{4}{3}$ or $C_A = 3$ respectively for incoming quarks (e.g. the Drell-Yan process) or incoming gluons (e.g. gluon induced Higgs production).

Next, we address the issue that gluons are not actually always emitted independently. This is already accounted for in Eq. (1) because, to order α_s^2 , the $M^2(k)$ quantity that appears there should be understood as an effective matrix element

$$\begin{aligned}[dk]M^2(k) &= [dk](M_1^2(k) + M_{1\text{-loop}}^2(k)) \\ &\quad + \int d^2k_t [dk_a][dk_b] M_{\text{correl}}^2(k_a, k_b) \delta^2(k_{t,ab} - k_t)\end{aligned}\quad (5)$$

where $M_1^2(k)$ is the pure $\mathcal{O}(\alpha_s)$ matrix element, $M_{\text{correl}}^2(k_a, k_b)$ is the correlated part of the matrix element for the emission of two soft-collinear gluons or a quark-antiquark pair, including relevant symmetry factors, and $M_{1\text{-loop}}^2$ is the corresponding part of the order α_s^2 1-loop matrix element. The separation into correlated and independent emissions is well defined because of the different colour factors that accompany them in the generic case [27–30]. The δ -function in the integral in Eq. (5) extracts the two-parton configurations with the same total transverse momentum as the 1-gluon configurations.

In the case of a jet veto, part of the result from the effective matrix element carries through as well: when the two correlated emissions are clustered into a single jet, it is the vectorial sum $k_{t,ab}$ of k_{ta} and k_{tb} that determines the jet transverse momentum. Therefore the same effective matrix element can be used in Eq. (2), as long as one includes an additional correction to account for configurations where the two emissions are clustered in separate jets:

$$\begin{aligned}\mathcal{F}^{\text{correl}} \sigma_0 &= \sigma_0 \int [dk_a][dk_b] M_{\text{correl}}^2(k_a, k_b) \times (1 - J(k_a, k_b)) \\ &\quad (\Theta(p_t^J - k_{ta})\Theta(p_t^J - k_{tb}) - \Theta(p_t^J - k_{t,ab})).\end{aligned}\quad (6)$$

At NNLL, $\mathcal{F}^{\text{correl}} = 4\alpha_s^2(p_{t,\text{veto}})CLf^{\text{correl}}(R)/\pi^2$ with

$$\begin{aligned}f^{\text{correl}}(R) &= \left(\frac{(-131 + 12\pi^2 + 132 \ln 2) C_A}{72} \right. \\ &\quad \left. + \frac{(23 - 24 \ln 2) n_f}{72} \right) \ln \frac{1}{R} + 0.61 C_A - 0.015 n_f + \mathcal{O}(R^2),\end{aligned}\quad (7)$$

for the generalised- k_t family of algorithms, in the limit of a small jet radius R . The R -independent terms have been determined numerically, while analytical terms up to R^6 , used in the rest of this article, and a full numerical result are to be found in [18]. Ref. [18] did not, however, make the relation with the boson p_t resummation.

All remaining contributions to a NNLL resummation, such as the 3-loop cusp anomalous dimension or a multiplicative $C_1 \alpha_s$ term are either purely virtual, and so independent of the precise observable, or involve at most

a single real emission, and so can be taken directly from the boson p_t resummations [5–8].¹ Thus the full NNLL resummed cross section for the jet-veto is given by:

$$\begin{aligned} \Sigma_{\text{NNLL}}^{(J)}(p_{t,\text{veto}}) = & \sum_{i,j} \int dx_1 dx_2 |\mathcal{M}_B|^2 \delta(x_1 x_2 s - M^2) \\ & \times \left[f_i(x_1, e^{-L} \mu_F) f_j(x_2, e^{-L} \mu_F) \left(1 + \frac{\alpha_s}{2\pi} \mathcal{H}^{(1)} \right) + \right. \\ & + \frac{\alpha_s}{2\pi} \frac{1}{1 - 2\alpha_s \beta_0 L} \sum_k \int_{x_1}^1 \frac{dz}{z} \left(C_{ki}^{(1)}(x_1) f_i\left(\frac{x_1}{z}, e^{-L} \mu_F\right) \right. \\ & \times \left. f_j(x_2, e^{-L} \mu_F) + \{(x_1, i) \leftrightarrow (x_2, j)\} \right) \left. \right] \\ & (1 + \mathcal{F}^{\text{clust}} + \mathcal{F}^{\text{correl}}) \times e^{L g_1(\alpha_s L) + g_2(\alpha_s L) + \frac{\alpha_s}{\pi} g_3(\alpha_s L)}, \end{aligned} \quad (8)$$

where the coefficient functions $\mathcal{H}^{(1)}$ and $C_{ki}^{(1)}$, and resummation functions g_1 , g_2 and g_3 are those that were derived for the boson p_t^B resummation in [5, 6, 8] and are given for completeness in the supplemental material to this letter [32] together with further discussion on the connection to the boson p_t^B resummation. The results are expressed in terms of $L = \ln(Q/p_{t,\text{veto}})$, $\alpha_s \equiv \alpha_s(\mu_R)$ and the resummation, renormalisation and factorisation scales Q , μ_R and μ_F are to be chosen of order of the boson mass M .

One check of Eq. (8) is to take its expansion in powers of α_s . $\Sigma_{\text{NNLL}}^{(J)}(p_t) = \alpha_s^2 \sum_{n=0}^{\infty} \Sigma_{\text{NNLL},n}^{(J)}(p_t)$ and compare $d\Sigma_{\text{NNLL},2}^{(J)}(p_t)/d\ln p_t$ to the exact NLO Higgs+1 jet prediction [33–35] from MCFM [36], $d\Sigma_2^{(J)}(p_t)/d\ln p_t$. NNLL resummation implies control of terms $\alpha_s^2 L^3 \dots \alpha_s^2$ (constant terms) in this quantity and so the difference between MCFM and the 2nd order expansion of the resummation should vanish for large L , and indeed this is what we find within reasonable precision. The precision of the test can be increased if one considers the $\mathcal{O}(\alpha_s^2)$ difference between the jet and boson- p_t resummations, because this difference has fewer logarithms and so is numerically easier to determine in MCFM. It is predicted to be

$$\begin{aligned} \frac{d\Sigma_{\text{NNLL},2}^{(J)}(p_t)}{d\ln p_t} - \frac{d\Sigma_{\text{NNLL},2}^{(B)}(p_t)}{d\ln p_t} = \\ - \frac{4C\alpha_s^2\sigma_0}{\pi^2} (f^{\text{clust}}(R) + f^{\text{correl}}(R) + \zeta_3 C). \end{aligned} \quad (9)$$

This is compared to MCFM’s LO H+2-jet result in the upper panel of Fig. 1. One sees excellent agreement at small p_t between Eq. (9) and the MCFM results, for

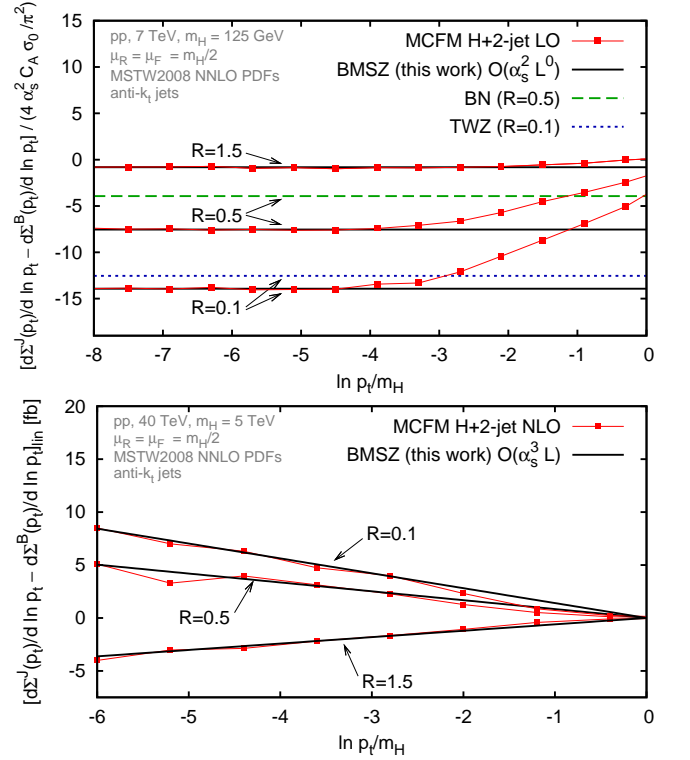


FIG. 1: Upper panel: the 2nd order difference between the jet and Higgs-boson $\ln p_t$ differential distributions, showing the coefficient of $4\alpha_s^2 C_A \sigma_0 / \pi^2$ as determined with MCFM and predicted in Eq. (9), for three R values. We also include comparisons with the prediction from [19] (BN) and a curve that includes the different $\mathcal{O}(1)$ terms claimed for $f^{\text{correl}}(R)$ in [64] (TWZ). Lower panel: the difference at $\mathcal{O}(\alpha_s^3 \sigma_0)$ between the jet and boson $\ln p_t$ differential distributions, with the expected $\alpha_s^3 \sigma_0 L^2$ term subtracted (as denoted by the subscript lin), showing the MCFM H+2-jet NLO result compared to our NNLL prediction for the $\alpha_s^3 \sigma_0 L$ term.

each of three R values. In contrast, the resummation of [19] (BN, shown just for $R = 0.5$) lacks the ζ_3 term in Eq. (9) and clearly does not agree with the MCFM results. Ref. [19] used a NNLL analysis of the $R \rightarrow \infty$ limit to relate jet and boson- p_t resummations. To correctly perform the $R \rightarrow \infty$ limit, one must however take into account a $N^3\text{LL}$ $\alpha_s^2 R$ term, which for $R \gtrsim \ln M/p_t$ is promoted to an additional NNLL $\alpha_s^2 \ln M/p_t$ contribution [32].

The above test can be extended one order further by examining the order $\alpha_s^3 \sigma_0$ difference between the jet and boson p_t differential distributions. The comparison between our predictions and the MCFM H+2-jet NLO result [39, 40] is given in the lower panel of Fig. 1. To facilitate the visual interpretation of the results, for each of the three R values the expected $\alpha_s^3 \sigma_0 L^2$ term has been subtracted. This should leave a pure $\alpha_s^3 \sigma_0 L$ term, for which our predictions and MCFM should be in accord. Such a term is indeed visible in the MCFM results and, within the fluctuations, appears to coincide well with our

¹ For resummations in generic processes, subtleties can arise with the spin-correlation effects discussed in [31]. These will generally be simpler in the case of jet vetoes, which don’t correlate distinct collinear regions.

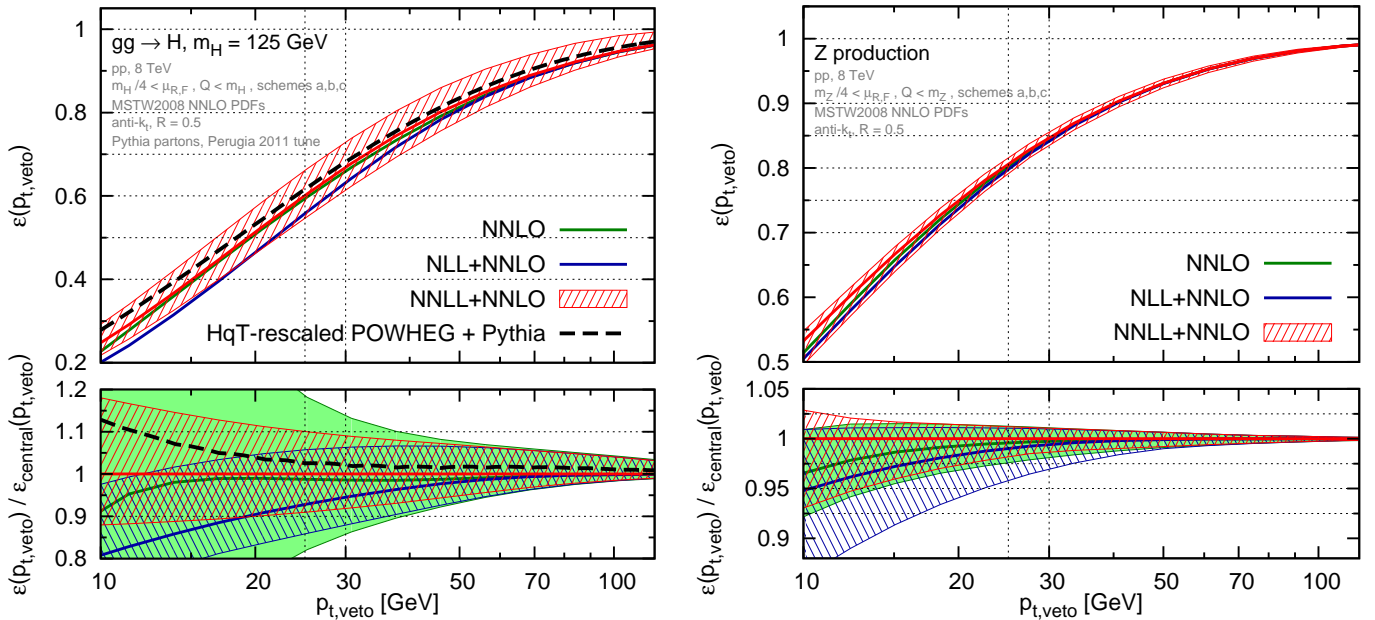


FIG. 2: Comparison of NNLO, NLL+NNLO and NNLL+NNLO results for the jet-veto efficiency for Higgs (left) and Z-boson (right) production at the LHC running at 8 TeV. The Higgs plot also includes the result from a POWHEG (revision 1683) [17, 37] plus Pythia (6.426) [14, 38] simulation in which the Higgs-boson p_t distribution has been reweighted to match the NNLL+NNLO prediction from HqT 2.0 [6] as in [18]. The lower panels show the results normalised to the central NNLL+NNLO curves.

predictions, providing a good degree of corroborating evidence for the correctness of our results beyond order $\alpha_s^2 \sigma_0$.

To illustrate the phenomenological implications of our work, we will show results for the jet veto efficiency $\epsilon(p_t) \equiv \Sigma^{(J)}(p_t)/\sigma_{\text{tot}}$, where σ_{tot} is the total cross section, known up to NNLO [41–46]. These results will combine (“match”) the resummed with fixed-order predictions, which can be taken from fully different NNLO boson-production calculations [3, 4, 47, 48] or from the NLO boson+jet calculations [33, 49] as implemented in MCFM [50]. We use three matching schemes, denoted by a , b and c , which are straightforward extensions of those used at NLL in [18], detailed in [32].

Our central predictions will be obtained by setting $\mu_R = \mu_F = Q = M/2$ and scheme a matching, with MSTW2008NNLO PDFs [51]. We use the anti- k_t [26] jet-algorithm with $R = 0.5$, as implemented in FastJet [52]. For the Higgs case we use the large m_{top} approximation and ignore $b\bar{b}$ fusion and b ’s in the $gg \rightarrow H$ loops (corrections beyond this approximation have a relevant impact, see [13, 53]). To determine uncertainties we consider variations of μ_R and μ_F by a factor of two in either direction, requiring $1/2 \leq \mu_R/\mu_F \leq 2$. Maintaining central $\mu_{R,F}$ values, we also examine variations of Q by a factor of two and the impact of changing matching scheme. Our final uncertainty band will be given by the envelope of all these variations. In the fixed-order results that we compare to, the band will just be the envelope of $\mu_{R,F}$ variations.

The results for the jet-veto efficiency in Higgs and Z-

boson production are shown in Fig. 2 for 8 TeV LHC collisions. Compared to the pure NNLO results, the central value is slightly higher and for Higgs production, the uncertainties are reduced, especially for lower $p_{t,\text{veto}}$ values. Compared to the NNLO+NLL results of [18] our central values are higher, sometimes close to edge of the NNLO+NLL uncertainty bands; since the NNLO+NLL results used the same approach for estimating the uncertainties, this suggests that that approach was not unduly conservative. In the Higgs case, the NNLO+NNLL uncertainty band is not particularly smaller than the NNLO+NLL one. This should not be a surprise, since [18] highlighted the existence of possible substantial corrections beyond NNLL and beyond NNLO. For the Higgs case, we also show a prediction from POWHEG [17, 37] interfaced to Pythia 6.4 [14] at parton level (Perugia 2011 shower tune [38]), reweighted so as to describe the NNLL+NNLO Higgs-boson p_t distribution from HqT (v2.0) [6], as used by the LHC experiments. While the reweighting procedure fails to provide NNLO or NNLL accuracy for the jet veto, for $p_{t,\text{veto}}$ scales of practical relevance, the result nevertheless agrees well with our central prediction. (Note also that it is harder to reliably estimate the uncertainties in a reweighting approach than in a direct calculation of the jet veto efficiency.)

For completeness, we provide here our central results and uncertainties for the jet-veto efficiencies and 0-jet cross sections (in pb) with the cuts (in GeV) used respectively by ATLAS and CMS, as well as results for a larger R value:

R	$p_{t,\text{veto}}$	$\epsilon(7 \text{ TeV})$	$\sigma_{0\text{-jet}}^{(7 \text{ TeV})}$	$\epsilon(8 \text{ TeV})$	$\sigma_{0\text{-jet}}^{(8 \text{ TeV})}$
0.4	25	$0.63^{+0.07}_{-0.05}$	$9.6^{+1.3}_{-1.1}$	$0.61^{+0.07}_{-0.06}$	$12.0^{+1.6}_{-1.4}$
0.5	30	$0.68^{+0.06}_{-0.05}$	$10.4^{+1.2}_{-1.1}$	$0.67^{+0.06}_{-0.05}$	$13.0^{+1.5}_{-1.5}$
1.0	30	$0.64^{+0.03}_{-0.05}$	$9.8^{+0.8}_{-1.1}$	$0.63^{+0.04}_{-0.05}$	$12.2^{+1.1}_{-1.4}$

Interestingly, the $R = 1$ results have a noticeably reduced upper uncertainty, due perhaps to the smaller value of the NNLL $f(R)$ correction (a large $f(R)$ introduces a significant Q -scale dependence). Note that the above results are without a rapidity cut on the jets; the actual rapidity cuts used by ATLAS and CMS lead only to small, $< 1\%$, differences [18].

To obtain the 0-jet cross sections above, we have used total cross sections at 7 TeV and 8 TeV of $15.3^{+1.1}_{-1.2}$ pb and $19.5^{+1.4}_{-1.5}$ pb respectively [54, 55] (based on results including [42–46]) and taken their scale uncertainties to be uncorrelated with those of the efficiencies. Symmetrising the uncertainties, we find a correlation coefficient between the 0-jet and ≥ 1 -jet cross sections of -0.43 and -0.50 for the $R = 0.4$ and $R = 0.5$ cases respectively,

using the covariance matrix as given in [32].

The code to perform the resummations and matchings shown here will be made publicly available in due course.

This work was supported by the UK STFC, the Agence Nationale de la Recherche under contract ANR-09-BLAN-0060, the Swiss National Science Foundation (SNF) under grant 200020-138206 and the European Commission under contract PITN-GA-2010-264564. We thank M. Grazzini and T. Gehrmann for helpful discussions and gratefully acknowledge exchanges with T. Becher and M. Neubert.

Note added: as our manuscript was being finalised, Ref. [64] appeared with the statement that the constants in Eq. (7) are wrong, claiming that our Ref. [18] incorrectly used the collinear limit of the correlated two-gluon and $q\bar{q}$ soft matrix elements. That claim is mistaken insofar as Ref. [18] used the full matrix elements from [27–30]. The constant terms suggested in [64] lead to the result labelled TWZ in Fig. 1 (upper) and appear to be inconsistent with the MCFM results.

-
- [1] S. Chatrchyan *et al.* [CMS Collaboration], arXiv:1202.1489 [hep-ex].
 - [2] G. Aad *et al.* [ATLAS Collaboration], arXiv:1206.0756 [hep-ex].
 - [3] C. Anastasiou, K. Melnikov, F. Petriello, Nucl. Phys. **B724** (2005) 197–246. [hep-ph/0501130].
 - [4] S. Catani and M. Grazzini, Phys. Rev. Lett. **98** (2007) 222002 [hep-ph/0703012]; M. Grazzini, JHEP **0802** (2008) 043. [arXiv:0801.3232 [hep-ph]].
 - [5] G. Bozzi, S. Catani, D. de Florian and M. Grazzini, Phys. Lett. B **564** (2003) 65 [arXiv:hep-ph/0302104].
 - [6] G. Bozzi, S. Catani, D. de Florian and M. Grazzini, Nucl. Phys. B **737** (2006) 73 [hep-ph/0508068].
 - [7] G. Bozzi, S. Catani, G. Ferrera, D. de Florian and M. Grazzini, Phys. Lett. B **696** (2011) 207 [arXiv:1007.2351 [hep-ph]].
 - [8] T. Becher and M. Neubert, Eur. Phys. J. C **71** (2011) 1665 [arXiv:1007.4005 [Hep-ph]].
 - [9] C. F. Berger, C. Marcantonini, I. W. Stewart, F. J. Tackmann and W. J. Waalewijn, JHEP **1104** (2011) 092 [arXiv:1012.4480 [hep-ph]].
 - [10] A. Banfi, M. Dasgupta and S. Marzani, Phys. Lett. B **701** (2011) 75 [arXiv:1102.3594 [hep-ph]].
 - [11] A. Banfi, M. Dasgupta, S. Marzani and L. Tomlinson, arXiv:1205.4760 [hep-ph].
 - [12] G. Davatz, F. Stockli, C. Anastasiou, G. Dissertori, M. Dittmar, K. Melnikov and F. Petriello, JHEP **0607** (2006) 037 [hep-ph/0604077].
 - [13] S. Dittmaier, C. Mariotti, G. Passarino, R. Tanaka, S. Alekhin, J. Alwall and E. A. Bagnaschi *et al.*, arXiv:1201.3084 [hep-ph].
 - [14] T. Sjostrand, S. Mrenna and P. Skands, JHEP **0605** (2006) 026 [arXiv:hep-ph/0603175].
 - [15] G. Corcella *et al.*, arXiv:hep-ph/0210213.
 - [16] S. Frixione and B. R. Webber, JHEP **0206** (2002) 029 [hep-ph/0204244].
 - [17] P. Nason, JHEP **0411** (2004) 040 [hep-ph/0409146].
 - [18] A. Banfi, G. P. Salam and G. Zanderighi, arXiv:1203.5773 [hep-ph].
 - [19] T. Becher and M. Neubert, arXiv:1205.3806 [hep-ph].
 - [20] G. Parisi and R. Petronzio, Nucl. Phys. B **154** (1979) 427.
 - [21] A. Banfi, G. P. Salam and G. Zanderighi, JHEP **0503** (2005) 073 [arXiv:hep-ph/0407286].
 - [22] S. Catani, Y. L. Dokshitzer, M. H. Seymour and B. R. Webber, Nucl. Phys. B **406** (1993) 187.
 - [23] S. D. Ellis and D. E. Soper, Phys. Rev. D **48**, 3160 (1993) [hep-ph/9305266].
 - [24] Y. L. Dokshitzer, G. D. Leder, S. Moretti and B. R. Webber, JHEP **9708**, 001 (1997) [hep-ph/9707323];
 - [25] M. Wobisch and T. Wengler, arXiv:hep-ph/9907280; M. Wobisch, DESY-THESIS-2000-049.
 - [26] M. Cacciari, G. P. Salam, G. Soyez, JHEP **0804** (2008) 063 [arXiv:0802.1189 [hep-ph]].
 - [27] F. A. Berends and W. T. Giele, Nucl. Phys. B **313** (1989) 595.
 - [28] Y. L. Dokshitzer, G. Marchesini and G. Orian, Nucl. Phys. B **387** (1992) 675.
 - [29] J. M. Campbell and E. W. N. Glover, Nucl. Phys. B **527** (1998) 264 [hep-ph/9710255].
 - [30] S. Catani and M. Grazzini, Nucl. Phys. B **570** (2000) 287 [hep-ph/9908523].
 - [31] S. Catani and M. Grazzini, Nucl. Phys. B **845** (2011) 297 [arXiv:1011.3918 [hep-ph]].
 - [32] A. Banfi, P. F. Monni, G. P. Salam and G. Zanderighi, supplemental material, available at the end of the arXiv version of this article.
 - [33] D. de Florian, M. Grazzini and Z. Kunszt, Phys. Rev. Lett. **82** (1999) 5209 [hep-ph/9902483].
 - [34] V. Ravindran, J. Smith and W. L. Van Neerven, Nucl. Phys. B **634** (2002) 247 [hep-ph/0201114].
 - [35] C. J. Glosser and C. R. Schmidt, JHEP **0212** (2002) 016

- [hep-ph/0209248].
- [36] J. M. Campbell and R. K. Ellis, Phys. Rev. D **65** (2002) 113007 [hep-ph/0202176].
 - [37] S. Alioli, P. Nason, C. Oleari and E. Re, JHEP **0904** (2009) 002 [arXiv:0812.0578 [hep-ph]].
 - [38] P. Z. Skands, Phys. Rev. D **82** (2010) 074018 [arXiv:1005.3457 [hep-ph]].
 - [39] J. M. Campbell, R. K. Ellis and G. Zanderighi, JHEP **0610** (2006) 028 [hep-ph/0608194].
 - [40] J. M. Campbell, R. K. Ellis and C. Williams, Phys. Rev. D **81** (2010) 074023 [arXiv:1001.4495 [hep-ph]].
 - [41] R. Hamberg, W. L. van Neerven and T. Matsuura, Nucl. Phys. B **359** (1991) 343 [Erratum-ibid. B **644** (2002) 403].
 - [42] S. Dawson, Nucl. Phys. B **359** (1991) 283.
 - [43] A. Djouadi, M. Spira and P. M. Zerwas, Phys. Lett. B **264** (1991) 440.
 - [44] R. V. Harlander and W. B. Kilgore, Phys. Rev. Lett. **88** (2002) 201801 [hep-ph/0201206].
 - [45] C. Anastasiou and K. Melnikov, Nucl. Phys. B **646** (2002) 220 [hep-ph/0207004].
 - [46] V. Ravindran, J. Smith and W. L. van Neerven, Nucl. Phys. B **665** (2003) 325 [hep-ph/0302135].
 - [47] K. Melnikov and F. Petriello, Phys. Rev. Lett. **96** (2006) 231803 [hep-ph/0603182].
 - [48] S. Catani, L. Cieri, G. Ferrera, D. de Florian, M. Grazzini, Phys. Rev. Lett. **103** (2009) 082001. [arXiv:0903.2120 [hep-ph]].
 - [49] W. T. Giele, E. W. N. Glover and D. A. Kosower, Nucl. Phys. B **403** (1993) 633 [hep-ph/9302225].
 - [50] J. M. Campbell and R. K. Ellis, Phys. Rev. D **60** (1999) 113006 [hep-ph/9905386].
 - [51] A. D. Martin, W. J. Stirling, R. S. Thorne, G. Watt, Eur. Phys. J. **C63** (2009) 189 [arXiv:0901.0002 [hep-ph]].
 - [52] M. Cacciari and G. P. Salam, Phys. Lett. B **641** (2006) 57 [arXiv:hep-ph/0512210]; M. Cacciari, G. P. Salam and G. Soyez, arXiv:1111.6097 [hep-ph].
 - [53] E. Bagnaschi, G. Degrandi, P. Slavich and A. Vicini, JHEP **1202** (2012) 088 [arXiv:1111.2854 [hep-ph]].
 - [54] S. Dittmaier *et al.* [LHC Higgs Cross Section Working Group Collaboration], arXiv:1101.0593 [hep-ph].
 - [55] D. de Florian and M. Grazzini, arXiv:1206.4133 [hep-ph].
 - [56] D. de Florian and M. Grazzini, Nucl. Phys. B **616** (2001) 247 [hep-ph/0108273].
 - [57] S. Moch, J. A. M. Vermaseren and A. Vogt, Nucl. Phys. B **688** (2004) 101 [hep-ph/0403192].
 - [58] W. Furmanski and R. Petronzio, Phys. Lett. B **97** (1980) 437.
 - [59] G. Curci, W. Furmanski and R. Petronzio, Nucl. Phys. B **175** (1980) 27.
 - [60] M. Dasgupta and G. P. Salam, JHEP **0208** (2002) 032 [arXiv:hep-ph/0208073].
 - [61] M. Cacciari and G. P. Salam, Phys. Lett. B **659** (2008) 119 [arXiv:0707.1378 [hep-ph]].
 - [62] J. M. Butterworth, A. R. Davison, M. Rubin and G. P. Salam, Phys. Rev. Lett. **100** (2008) 242001 [arXiv:0802.2470 [hep-ph]].
 - [63] D. Krohn, J. Thaler and L. -T. Wang, JHEP **1002** (2010) 084 [arXiv:0912.1342 [hep-ph]].
 - [64] F. J. Tackmann, J. R. Walsh and S. Zuberi, arXiv:1206.4312 [hep-ph].

Supplemental material

We here provide material that completes the discussion of the letter, including more explicit formulae, some derivations and supplementary figures.

1. Explicit resummation formulae

In the present section we report the explicit expressions for the resummation functions g_1 , g_2 and g_3 computed in [5, 6], as functions of $\lambda = \alpha_s \beta_0 L$, with $L = \ln(Q/p_t)$. α_s denotes $\alpha_s(\mu_R)$ unless otherwise stated, and Q is the resummation scale (see main text)

$$g_1(\lambda) = \frac{A^{(1)}}{\pi\beta_0} \frac{2\lambda + \ln(1-2\lambda)}{2\lambda}, \quad (10a)$$

$$g_2(\lambda) = \frac{1}{2\pi\beta_0} \ln(1-2\lambda) \left(A^{(1)} \ln \frac{M^2}{Q^2} + B^{(1)} \right) - \frac{A^{(2)}}{4\pi^2\beta_0^2} \frac{2\lambda + (1-2\lambda)\ln(1-2\lambda)}{1-2\lambda} \\ + A^{(1)} \left(-\frac{\beta_1}{4\pi\beta_0^3} \frac{\ln(1-2\lambda)((2\lambda-1)\ln(1-2\lambda)-2)-4\lambda}{1-2\lambda} - \frac{1}{2\pi\beta_0} \frac{(2\lambda(1-\ln(1-2\lambda))+\ln(1-2\lambda))}{1-2\lambda} \ln \frac{\mu_R^2}{Q^2} \right), \quad (10b)$$

$$g_3(\lambda) = \left(A^{(1)} \ln \frac{M^2}{Q^2} + B^{(1)} \right) \left(-\frac{\lambda}{1-2\lambda} \ln \frac{\mu_R^2}{Q^2} + \frac{\beta_1}{2\beta_0^2} \frac{2\lambda + \ln(1-2\lambda)}{1-2\lambda} \right) - \frac{1}{2\pi\beta_0} \frac{\lambda}{1-2\lambda} \left(A^{(2)} \ln \frac{M^2}{Q^2} + B^{(2)} \right) \\ - \frac{A^{(3)}}{4\pi^2\beta_0^2} \frac{\lambda^2}{(1-2\lambda)^2} + A^{(2)} \left(\frac{\beta_1}{4\pi\beta_0^3} \frac{2\lambda(3\lambda-1) + (4\lambda-1)\ln(1-2\lambda)}{(1-2\lambda)^2} - \frac{1}{\pi\beta_0} \frac{\lambda^2}{(1-2\lambda)^2} \ln \frac{\mu_R^2}{Q^2} \right) \\ + A^{(1)} \left(\frac{\lambda(\beta_0\beta_2(1-3\lambda) + \beta_1^2\lambda)}{\beta_0^4(1-2\lambda)^2} + \frac{(1-2\lambda)\ln(1-2\lambda)(\beta_0\beta_2(1-2\lambda) + 2\beta_1^2\lambda)}{2\beta_0^4(1-2\lambda)^2} + \frac{\beta_1^2}{4\beta_0^4} \frac{(1-4\lambda)\ln^2(1-2\lambda)}{(1-2\lambda)^2} \right. \\ \left. - \frac{\lambda^2}{(1-2\lambda)^2} \ln^2 \frac{\mu_R^2}{Q^2} - \frac{\beta_1}{2\beta_0^2} \frac{(2\lambda(1-2\lambda) + (1-4\lambda)\ln(1-2\lambda))}{(1-2\lambda)^2} \ln \frac{\mu_R^2}{Q^2} \right), \quad (10c)$$

where, for Higgs, $A^{(1)} = 2C_A$ and $B^{(1)} = -4\pi\beta_0$, while for Drell-Yan, $A^{(1)} = 2C_F$ and $B^{(1)} = -3C_F$. The remaining coefficients can be expressed in a unique way as [8, 56, 57]:

$$A^{(2)} = A^{(1)} K_{\text{CMW}}^{(1)}, \quad A^{(3)} = A^{(1)} K_{\text{CMW}}^{(2)} + \pi\beta_0 C d^{(2)}, \quad B^{(2)} = -2\gamma^{(2)} + 2\pi\beta_0 C \zeta_2, \quad (11)$$

$$\beta_0 = \frac{11C_A - 2n_f}{12\pi}, \quad \beta_1 = \frac{17C_A^2 - 5C_A n_f - 3C_F n_f}{24\pi^2}, \quad (12)$$

$$\beta_2 = \frac{2857C_A^3 + (54C_F^2 - 615C_F C_A - 1415C_A^2)n_f + (66C_F + 79C_A)n_f^2}{3456\pi^3}, \quad (13)$$

in terms of the Casimir $C = C_A$ for Higgs and $C = C_F$ for Drell-Yan, and of the well known constants

$$K_{\text{CMW}}^{(1)} = C_A \left(\frac{67}{18} - \frac{\pi^2}{6} \right) - \frac{5}{9}n_f, \quad d^{(2)} = C_A \left(\frac{808}{27} - 28\zeta_3 \right) - \frac{224}{54}n_f, \quad (14a)$$

$$K_{\text{CMW}}^{(2)} = C_A^2 \left(\frac{245}{24} - \frac{67}{9}\zeta_2 + \frac{11}{6}\zeta_3 + \frac{11}{5}\zeta_2^2 \right) + C_F n_f \left(-\frac{55}{24} + 2\zeta_3 \right) + C_A n_f \left(-\frac{209}{108} + \frac{10}{9}\zeta_2 - \frac{7}{3}\zeta_3 \right) - \frac{1}{27}n_f^2. \quad (14b)$$

Here $\gamma^{(2)}$ [58, 59] are the coefficients of the $\delta(1-z)$ term in the NLO splitting functions $P^{(1)}$. For Higgs production we have

$$\gamma^{(2)} = C_A^2 \left(\frac{8}{3} + 3\zeta_3 \right) - \frac{1}{2}C_F n_f - \frac{2}{3}C_A n_f, \quad (15)$$

whilst for the Drell-Yan process

$$\gamma^{(2)} = C_F^2 \left(\frac{3}{8} - \frac{\pi^2}{2} + 6\zeta_3 \right) + C_F C_A \left(\frac{17}{24} + \frac{11}{18}\pi^2 - 3\zeta_3 \right) - C_F n_f \left(\frac{1}{12} + \frac{\pi^2}{9} \right). \quad (16)$$

We finally report the expressions for the collinear coefficient function $C_{ij}^{(1)}(z)$ and the hard virtual term $\mathcal{H}^{(1)}$ in eq. (8)²

$$C_{ij}^{(1)}(z) = -P_{ij}^{(0),\epsilon}(z) - \delta_{ij}\delta(1-z)C\frac{\pi^2}{12} + P_{ij}^{(0)}(z)\ln\frac{Q^2}{\mu_F^2}, \quad (17a)$$

$$\mathcal{H}^{(1)} = H^{(1)} - \left(B^{(1)} + \frac{A^{(1)}}{2}\ln\frac{M^2}{Q^2}\right)\ln\frac{M^2}{Q^2} + q\,2\pi\beta_0\ln\frac{\mu_R^2}{M^2}, \quad (17b)$$

where q is the α_s power of the LO cross section ($q = 2$ for Higgs production and $q = 0$ for Drell-Yan). The coefficient $H^{(1)}$ encodes the pure hard virtual correction to the leading order process, it is given by

$$\text{Higgs :} \quad H^{(1)} = C_A \left(5 + \frac{7}{6}\pi^2\right) - 3C_F, \quad (18a)$$

$$\text{Drell - Yan :} \quad H^{(1)} = C_F \left(-8 + \frac{7}{6}\pi^2\right). \quad (18b)$$

Finally, $P_{ij}^{(0),\epsilon}(z)$ is the $\mathcal{O}(\epsilon)$ term of the LO splitting function $P_{ij}^{(0)}(z)$:

$$P_{qq}^{(0),\epsilon}(z) = -C_F(1-z), \quad (19a)$$

$$P_{gq}^{(0),\epsilon}(z) = -C_F z, \quad (19b)$$

$$P_{qg}^{(0),\epsilon}(z) = -z(1-z), \quad (19c)$$

$$P_{gg}^{(0),\epsilon}(z) = 0. \quad (19d)$$

2. Full matching formulae

We start by recalling the three prescriptions discussed in [18] for defining the jet-veto efficiency at NNLO accuracy. In this section, in order to simplify the notation, we will refer to the integrated jet-veto distribution $\Sigma^{(J)}$ as Σ .

$$\epsilon^{(a)}(p_{t,\text{veto}}) = \frac{\Sigma_0(p_{t,\text{veto}}) + \Sigma_1(p_{t,\text{veto}}) + \Sigma_2(p_{t,\text{veto}})}{\sigma_0 + \sigma_1 + \sigma_2}, \quad (20a)$$

$$\epsilon^{(b)}(p_{t,\text{veto}}) = \frac{\Sigma_0(p_{t,\text{veto}}) + \Sigma_1(p_{t,\text{veto}}) + \bar{\Sigma}_2^{(J)}(p_{t,\text{veto}})}{\sigma_0 + \sigma_1}, \quad (20b)$$

$$\epsilon^{(c)}(p_{t,\text{veto}}) = 1 + \frac{\bar{\Sigma}_1^{(J)}(p_{t,\text{veto}})}{\sigma_0} - \frac{\sigma_1}{\sigma_0^2}\bar{\Sigma}_1^{(J)}(p_{t,\text{veto}}) + \frac{\bar{\Sigma}_2^{(J)}(p_{t,\text{veto}})}{\sigma_0} \quad (20c)$$

with

$$\Sigma_i(p_{t,\text{veto}}) = \sigma_i + \bar{\Sigma}_i^{(J)}(p_{t,\text{veto}}) \quad (21)$$

being the $\mathcal{O}(\alpha_s^i)$ -th correction relative to the Born cross section where

$$\bar{\Sigma}_i^{(J)}(p_{t,\text{veto}}) = - \int_{p_{t,\text{veto}}}^{\infty} dp_t \frac{d\Sigma_i(p_t)}{dp_t}, \quad (22)$$

can be determined from MCFM, while σ_i is the i^{th} order contribution to the total cross section (cf. [41–46]). The above three prescriptions differ by terms $\mathcal{O}(\alpha_s^3)$, which are beyond the control of current fixed-order calculations.

² Often in the literature, the hard coefficient $H^{(1)}$ is considered as part of the $\delta(1-z)$ term in the coefficient function $C_{ij}^{(1)}(z)$, so it comes with a factor $1/(1 - \alpha_s\beta_0 L)$ in eq. (8). This results in a different convention for the resummation coefficient $B^{(2)}$ which will differ by an amount $2\pi\beta_0 H^{(1)}$ from what reported here.

The jet-veto matched efficiency should tend to one and the differential distribution should vanish at the maximum allowed transverse momentum $p_{t,\text{veto}}^{\text{max}}$

$$\epsilon(p_{t,\text{veto}}^{\text{max}}) = 1, \quad \frac{d\epsilon}{dp_{t,\text{veto}}}(p_{t,\text{veto}}^{\text{max}}) = 0. \quad (23)$$

To fulfil such requirements, we modify the resummed logarithms as follows

$$L \rightarrow \tilde{L} = \left(1 - \frac{p_{t,\text{veto}}}{p_{t,\text{veto}}^{\text{max}}}\right) \frac{1}{p} \ln \left(\left(\frac{Q}{p_{t,\text{veto}}}\right)^p - \left(\frac{Q}{p_{t,\text{veto}}^{\text{max}}}\right)^p + 1 \right), \quad (24)$$

where p is some integer power. By default we choose $p = 5$ [18]. The factor $\left(1 - \frac{p_{t,\text{veto}}}{p_{t,\text{veto}}^{\text{max}}}\right)$ is necessary to fulfil eq. (23) but it is largely irrelevant in practice since $p_{t,\text{veto}}^{\text{max}}$ is much larger than the typical values of the jet transverse momentum veto (in practice, we set $p_{t,\text{max}} = \infty$). We introduce three multiplicative matching schemes [60], each of them corresponding to one of the three efficiency definitions (20a), (20b), (20c). To simplify the notation, we split the luminosity factor in the square brackets of Eq. (8) into two terms $\mathcal{L}^{(0)}(\tilde{L})$ and $\mathcal{L}^{(1)}(\tilde{L})$, which start at order α_s^0 and α_s^1 respectively,

$$\mathcal{L}^{(0)}(\tilde{L}) = \sum_{i,j} \int dx_1 dx_2 \delta(x_1 x_2 s - M^2) f_i(x_1, e^{-\tilde{L}} \mu_F) f_j(x_2, e^{-\tilde{L}} \mu_F), \quad (25)$$

$$\begin{aligned} \mathcal{L}^{(1)}(\tilde{L}) = & \frac{\alpha_s}{2\pi} \sum_{i,j} \int dx_1 dx_2 \delta(x_1 x_2 s - M^2) \left[f_i(x_1, e^{-\tilde{L}} \mu_F) f_j(x_2, e^{-\tilde{L}} \mu_F) \mathcal{H}^{(1)} \right. \\ & \left. + \frac{1}{1 - 2\alpha_s \beta_0 \tilde{L}} \sum_k \left(\int_{x_1}^1 \frac{dz}{z} C_{ki}^{(1)}(z) f_i\left(\frac{x_1}{z}, e^{-\tilde{L}} \mu_F\right) f_j(x_2, e^{-\tilde{L}} \mu_F) + \{(x_1, i) \leftrightarrow (x_2, j)\} \right) \right]. \end{aligned} \quad (26)$$

The first of the three matching schemes then reads

$$\begin{aligned} \Sigma_{\text{matched}}^{(a)}(p_{t,\text{veto}}) = & \frac{1}{\sigma_0} \frac{\Sigma_{\text{NNLL}}(p_{t,\text{veto}})}{1 + \mathcal{L}^{(1)}(\tilde{L})/\mathcal{L}^{(0)}(\tilde{L})} \left[\sigma_0 \left(1 + \frac{\mathcal{L}^{(1)}(\tilde{L})}{\mathcal{L}^{(0)}(\tilde{L})} \right) + \Sigma^{(1)}(p_{t,\text{veto}}) - \Sigma_{\text{NNLL}}^{(1)}(p_{t,\text{veto}}) \right. \\ & \left. + \Sigma^{(2)}(p_{t,\text{veto}}) - \Sigma_{\text{NNLL}}^{(2)}(p_{t,\text{veto}}) + \left(\frac{\mathcal{L}^{(1)}(0)}{\mathcal{L}^{(0)}(0)} - \frac{\Sigma_{\text{NNLL}}^{(1)}(p_{t,\text{veto}})}{\sigma_0} \right) \left(\Sigma^{(1)}(p_{t,\text{veto}}) - \Sigma_{\text{NNLL}}^{(1)}(p_{t,\text{veto}}) \right) \right], \end{aligned} \quad (27)$$

and the corresponding jet-veto efficiency is

$$\epsilon_{\text{matched}}^{(a)}(p_{t,\text{veto}}) = \frac{\Sigma_{\text{matched}}^{(a)}(p_{t,\text{veto}})}{\Sigma_{\text{matched}}^{(a)}(p_{t,\text{veto}}^{\text{max}})}. \quad (28)$$

The second scheme can be derived from the previous one by replacing $\Sigma^{(2)}(p_{t,\text{veto}})$ with $\bar{\Sigma}^{(2)}(p_{t,\text{veto}})$. For the vetoed cross section we get

$$\begin{aligned} \Sigma_{\text{matched}}^{(b)}(p_{t,\text{veto}}) = & \frac{1}{\sigma_0} \frac{\Sigma_{\text{NNLL}}(p_{t,\text{veto}})}{1 + \mathcal{L}^{(1)}(\tilde{L})/\mathcal{L}^{(0)}(\tilde{L})} \left[\sigma_0 \left(1 + \frac{\mathcal{L}^{(1)}(\tilde{L})}{\mathcal{L}^{(0)}(\tilde{L})} \right) + \Sigma^{(1)}(p_{t,\text{veto}}) - \Sigma_{\text{NNLL}}^{(1)}(p_{t,\text{veto}}) \right. \\ & \left. + \bar{\Sigma}^{(2)}(p_{t,\text{veto}}) - \Sigma_{\text{NNLL}}^{(2)}(p_{t,\text{veto}}) + \left(\frac{\mathcal{L}^{(1)}(0)}{\mathcal{L}^{(0)}(0)} - \frac{\Sigma_{\text{NNLL}}^{(1)}(p_{t,\text{veto}})}{\sigma_0} \right) \left(\Sigma^{(1)}(p_{t,\text{veto}}) - \Sigma_{\text{NNLL}}^{(1)}(p_{t,\text{veto}}) \right) \right], \end{aligned} \quad (29)$$

while for its efficiency

$$\epsilon_{\text{matched}}^{(b)}(p_{t,\text{veto}}) = \frac{\Sigma_{\text{matched}}^{(b)}(p_{t,\text{veto}})}{\Sigma_{\text{matched}}^{(b)}(p_{t,\text{veto}}^{\text{max}})}. \quad (30)$$

Finally, the third matching scheme is directly formulated for the efficiency resulting in

$$\begin{aligned} \epsilon_{\text{matched}}^{(c)}(p_{t,\text{veto}}) = & \frac{1}{\sigma_0^2} \frac{\Sigma_{\text{NNLL}}(p_{t,\text{veto}})}{1 + \mathcal{L}^{(1)}(\tilde{L})/\mathcal{L}^{(0)}(\tilde{L})} \left[\sigma_0 \left(1 + \frac{\mathcal{L}^{(1)}(\tilde{L})}{\mathcal{L}^{(0)}(\tilde{L})} \right) + \bar{\Sigma}^{(1)}(p_{t,\text{veto}}) - \Sigma_{\text{NNLL}}^{(1)}(p_{t,\text{veto}}) \right. \\ & + \bar{\Sigma}^{(2)}(p_{t,\text{veto}}) - \frac{\sigma_1}{\sigma_0} \bar{\Sigma}^{(1)}(p_{t,\text{veto}}) - \Sigma_{\text{NNLL}}^{(2)}(p_{t,\text{veto}}) \\ & \left. + \left(\frac{\mathcal{L}^{(1)}(0)}{\mathcal{L}^{(0)}(0)} - \frac{\Sigma_{\text{NNLL}}^{(1)}(p_{t,\text{veto}})}{\sigma_0} \right) \left(\bar{\Sigma}^{(1)}(p_{t,\text{veto}}) - \Sigma_{\text{NNLL}}^{(1)}(p_{t,\text{veto}}) \right) \right]. \quad (31) \end{aligned}$$

3. Details of relation between jet and boson- p_t resummations

This section collects a number of results to help relate jet and boson p_t resummations. Firstly we demonstrate that the $g_n(\alpha_s L)$ from a boson p_t resummation can be directly carried over to jet p_t resummation for $n \leq 3$. Then we obtain a form for the boson p_t resummation that is suitable for expansion and comparison with fixed-order results. Finally we consider the large R limit of the jet- p_t resummation, which was used in [19] to attempt to obtain a relation between jet and boson p_t resummations.

a. Relating $g_n(\alpha_s L)$ between boson and jet resummations

One of the main ingredients of our results are the $g_n(\alpha_s L)$ functions that are used in boson p_t resummations. These stem from the rightmost integral in Eq. (1), which involves a Fourier transformation, whereas in Eq. (2) we need related integrals but with a theta-function instead of the $(\exp(ib \cdot k_t) - 1)$ factor.

We start from the expression for the resummed p_t distribution in eq. (1) and concentrate on the part of the matrix-element in the right-hand integral that is responsible for the leading logarithms. Integrating over azimuthal angles we obtain:

$$\frac{d\Sigma^{(B)}(p_t)}{p_t dp_t} = \sigma_0 \int b db J_0(bp_t) \exp[-\mathcal{R}(b)], \quad \mathcal{R}(b) = \int [dk] M^2(k) (1 - J_0(bk_t)). \quad (32)$$

We wish to show that we can safely perform the replacement

$$(1 - J_0(bk_t)) \rightarrow \Theta(k_t - b_0/b), \quad b_0 = 2e^{-\gamma_E}, \quad (33)$$

up to and including NNLL accuracy. Integrating over rapidity $\mathcal{R}(b)$ has the form

$$\mathcal{R}(b) = \int_0^M \frac{dk_t}{k_t} F\left(\alpha_s \ln \frac{M}{k_t}\right) (1 - J_0(bk_t)), \quad F\left(\alpha_s \ln \frac{M}{k_t}\right) = 4C \frac{\alpha_s}{\pi} \ln \frac{M}{k_t} \frac{1}{1 - 2\alpha_s \beta_0 \ln \frac{M}{k_t}}. \quad (34)$$

To evaluate separately real and virtual contributions in eq. (34), we introduce a dimensional regulator and write

$$\mathcal{R}(b) = F(\alpha_s \partial_\epsilon) \int_0^M \frac{dk_t}{k_t} \left(\frac{k_t}{M} \right)^{-\epsilon} (1 - J_0(bk_t)) \Big|_{\epsilon=0}, \quad (35)$$

which yields

$$\mathcal{R}(b) = R_{\text{LL}}(b_0/b) + \delta\mathcal{R}(b), \quad (36)$$

where, neglecting terms suppressed by powers of $1/(bM)$,

$$R_{\text{LL}}(b_0/b) = \int_0^M \frac{dk_t}{k_t} F\left(\alpha_s \ln \frac{M}{k_t}\right) \Theta(k_t - b_0/b), \quad (37)$$

and

$$\delta\mathcal{R}(b) = F(\alpha_s \partial_\epsilon) \frac{(b/b_0)^\epsilon}{\epsilon} \left[-1 + e^{-\gamma_E \epsilon} \frac{\Gamma(1 - \frac{\epsilon}{2})}{\Gamma(1 + \frac{\epsilon}{2})} \right] \Big|_{\epsilon=0} \quad (38a)$$

$$= F(\alpha_s \partial_\epsilon) \left(\frac{b}{b_0} \right)^\epsilon \left[\frac{\zeta_3}{12} \epsilon^2 + \mathcal{O}(\epsilon^4) \right] \Big|_{\epsilon=0}. \quad (38b)$$

This gives at most a term $\alpha_s^n \ln^{n-2}(Mb/b_0)$, i.e. a N³LL term. A similar argument can be applied to contributions to $\mathcal{R}(b)$ arising from less singular regions, giving also rise to terms that are beyond NNLL. Consequently, to NNLL accuracy, the same g_1 , g_2 and g_3 functions can be used in both the jet and boson resummation.

b. Evaluation of the boson- p_t integrated cross section

To facilitate comparisons between the jet and boson p_t resummations at fixed order, it is convenient to have an expression for the boson p_t resummation whose fixed-order expansion can be straightforwardly obtained. The full expression for the cumulative p_t cross section can be found in [5, 6, 8] and reads

$$\Sigma^{(B)}(p_t) = \int_0^\infty dy J_1(y) |\mathcal{M}_B|^2 e^{-R(b_0/b)} \left(\mathcal{L}^{(0)}(\ln(Qb/b_0)) + \mathcal{L}^{(1)}(\ln(Qb/b_0)) \right), \quad (39)$$

where

$$-R(b_0/b) = \ln(Qb/b_0)g_1(\alpha_s \ln(Qb/b_0)) + g_2(\alpha_s \ln(Qb/b_0)) + \frac{\alpha_s}{\pi}g_3(\alpha_s \ln(Qb/b_0)) \quad (40)$$

is the full NNLL radiator. As discussed above, the resummation functions g_1 , g_2 and g_3 are those used for the jet veto case. To perform the inverse Fourier transform we expand $R(b_0/b)$ and the full luminosity factor around $b = b_0/p_t$ and neglect subleading logarithmic terms getting, at NNLL accuracy,

$$\begin{aligned} \Sigma^{(B)}(p_t) = \int_0^\infty dy J_1(y) |\mathcal{M}_B|^2 & \left[\mathcal{L}^{(0)}(\ln(Q/p_t)) + \mathcal{L}^{(1)}(\ln(Q/p_t)) + \partial_{\ln p_t} \mathcal{L}^{(0)}(\ln(Q/p_t)) \ln(y/b_0) \right] \\ & \times \left(\frac{y}{b_0} \right)^{-R'} e^{-R(p_t)} \left(1 - \frac{1}{2} R'' \ln^2(y/b_0) \right), \end{aligned} \quad (41)$$

where we have performed the change of variable $y = bp_t$, and we have made use of R' and R'' , the first and second derivatives of R with respect to $\ln(Q/p_t)$. To order $\alpha_s L$, $R' = 4\alpha_s C \ln(Q/p_t)/\pi$. Moreover, from eq. (25), we see that the variation of $\mathcal{L}^{(0)}(L)$ reads

$$\partial_{\ln p_t} \mathcal{L}^{(0)}(L) = \frac{\alpha_s}{\pi} \sum_{i,j,k} \int dx_1 dx_2 \delta(x_1 x_2 s - M^2) \left[(P_{ki}^{(0)} \otimes f_i)(x_1, e^{-L} \mu_F) f_j(x_2, e^{-L} \mu_F) + \{(x_1, i) \leftrightarrow (x_2, j)\} \right]. \quad (42)$$

It is straightforward to show that eq. (41) evaluates to

$$\begin{aligned} \Sigma^{(B)}(p_t) = |\mathcal{M}_B|^2 e^{-R(p_t)} & \left[\mathcal{L}^{(0)}(\ln(Q/p_t)) \left(1 - \frac{1}{2} R'' \partial_{R'}^2 \right) \right. \\ & \left. + \mathcal{L}^{(1)}(\ln(Q/p_t)) - \partial_{\ln p_t} \mathcal{L}^{(0)}(\ln(Q/p_t)) \partial_{R'} \right] e^{-\gamma_E R'} \frac{\Gamma(1 - \frac{R'}{2})}{\Gamma(1 + \frac{R'}{2})}. \end{aligned} \quad (43)$$

In this notation, the result for the jet-veto cross section is simply $|\mathcal{M}_B|^2 e^{-R(p_t)} (\mathcal{L}^{(0)} + \mathcal{L}^{(1)}) (1 + \mathcal{F}^{\text{clust}} + \mathcal{F}^{\text{correl}})$. It is therefore immediate to evaluate the differences between the two formulae at any given fixed order and in particular to derive Eq. (9): making use of the fact that $e^{-\gamma_E R'} \Gamma(1 - \frac{R'}{2}) / \Gamma(1 + \frac{R'}{2})$ has an expansion of the form $1 + \frac{\zeta_3}{12} R'^3 + \mathcal{O}(R'^5)$, one sees that the only terms in the difference that survive at order $\alpha_s^2 L$ are the $\mathcal{F}^{\text{clust}}$ and $\mathcal{F}^{\text{correl}}$ contributions and the $R'' \partial_{R'}^2$ term of Eq. (43), with the latter giving

$$-\sigma_0 \frac{1}{2} R'' \partial_{R'}^2 e^{-\gamma_E R'} \frac{\Gamma(1 - \frac{R'}{2})}{\Gamma(1 + \frac{R'}{2})} = \sigma_0 \left(-4 \frac{\alpha_s^2}{\pi^2} \zeta_3 C^2 \ln \frac{Q}{p_t} + \mathcal{O}(\alpha_s^2 L^0) + \mathcal{O}(\alpha_s^3 L^2) \right), \quad (44)$$

which is the source of the ζ_3 in Eq. (9).³

³ One point to note in evaluating the difference between the jet and boson p_t resummations at order $\alpha_s^3 L^2$ is that it is necessary to account also for the difference between C_2 terms for the two resummations. One of the properties of this difference of C_2 terms is that it has Q dependence that ensures that the final prediction for the difference of $\alpha_s^3 L^2$ terms is Q -independent. To produce figure 1 the difference of C_2 terms was taken from a numerical determination based on the MCFM leading-order $H + 2$ -jet calculation.

c. Use of the large- R limit to relate boson and jet- p_t resummations

One natural way of relating jet and boson- p_t resummations is to make the observation that for an infinite jet radius, all partons will be clustered into a single jet, which will have a transverse momentum that balances exactly that of the boson. This approach was taken in Ref. [19] and here we examine it in detail.

First, let us consider the properties of $\mathcal{F}^{\text{clust}}$ and $\mathcal{F}^{\text{correl}}$ for large R . It is straightforward to see that $\mathcal{F}^{\text{correl}}$ vanishes for large R , since in Eq. (7) the two partons will always be clustered together, giving $1 - J(k_1, k_2) = 0$. For $\mathcal{F}^{\text{clust}}$, the NNLL component for $R > \pi$ can be evaluated in closed form and is given by

$$\mathcal{F}^{\text{clust}} = -R'_B \frac{\alpha_s(p_{t,\text{veto}})C}{\pi} \left(\left(\frac{\pi}{6} R^2 - \frac{R^4}{8\pi} \right) \arctan \frac{\pi}{\sqrt{R^2 - \pi^2}} + \left(\frac{R^2}{8} - \frac{\pi^2}{12} \right) \sqrt{R^2 - \pi^2} \right). \quad (45)$$

This has the property that it vanishes as $1/R$ for large R . Thus it would appear that at order $\alpha_s^2 L$ the difference between jet and boson- p_t resummations should be given by [19]

$$\frac{d\Sigma_{\text{NNLL},2}^{(J)}(p_t)}{d \ln p_t} - \frac{d\Sigma_{\text{NNLL},2}^{(B)}(p_t)}{d \ln p_t} = (f(R) - f(\infty)) \alpha_s^2 \sigma_0 = f(R) \alpha_s^2 \sigma_0, \quad (46)$$

which differs from the result in Eq. (9) (here $f(R) = f^{\text{correl}}(R) + f^{\text{clust}}(R)$).

To understand the origin of this difference, it is helpful to examine the structures that lead to $\mathcal{F}^{\text{clust}}$ vanishing for large R . A first observation is that for large R , $J(k_1, k_2)$ can be written as

$$J(k_1, k_2) = \Theta \left(R - |\Delta y| + \frac{\Delta \phi^2}{2R} + \mathcal{O} \left(\frac{1}{R^3} \right) \right), \quad \Delta y \equiv y_1 - y_2, \quad \Delta \phi = \phi_1 - \phi_2. \quad (47)$$

Neglecting the term of order $1/R$ will allow us to simplify our discussion and so we will instead examine a “rapidity-only” jet algorithm with the clustering function

$$J_{\text{rap}}(k_1, k_2) = \Theta(R - |\Delta y|). \quad (48)$$

Let us now evaluate Eq. (3) with J_{rap} . We break the problem into rapidity, transverse momentum and azimuthal integrals. Each emission i is limited to a rapidity $|y_i| < \ln(M/k_{ti})$. Assuming that we can neglect terms $\ln(k_{t1}/k_{t2})$ from the rapidity integration, we can write the latter as

$$\int dy_1 dy_2 \Theta \left(|y_1| - \ln \frac{M}{k_{t1}} \right) \Theta \left(|y_2| - \ln \frac{M}{k_{t2}} \right) \Theta(R - |y_1 - y_2|) = 4R \ln \frac{M}{k_{t1}} - R^2 + \mathcal{O}(R \ln \zeta), \quad (49)$$

where $\zeta = k_{t2}/k_{t1}$ and we have included the constraint that $J_{\text{rap}}(k_1, k_2)$ be non-zero. We can then write Eq. (3) as

$$\mathcal{F}^{\text{clust}} = 16 \frac{\alpha_s^2 C^2}{\pi^2} \int_0^1 \frac{d\zeta}{\zeta} \int_{-\pi}^{\pi} \frac{d\phi}{2\pi} \int_{p_t}^{\frac{p_t}{\sqrt{1+\zeta^2+2\zeta \cos \phi}}} \frac{dk_{t,1}}{k_{t,1}} \left(4R \ln \frac{M}{k_{t1}} - R^2 \right), \quad (50)$$

where we have dropped the $\mathcal{O}(R \ln \zeta)$ term of Eq. (49). Performing the k_{t1} integration gives

$$\mathcal{F}^{\text{clust}} = 16 \frac{\alpha_s^2 C^2}{\pi^2} \int_0^1 \frac{d\zeta}{\zeta} \int_{-\pi}^{\pi} \frac{d\phi}{2\pi} \left[\left(-2R \ln \frac{M}{p_t} + \frac{R^2}{2} \right) \ln(1 + \zeta^2 + 2\zeta \cos \phi) - \frac{R}{2} \ln^2(1 + \zeta^2 + 2\zeta \cos \phi) \right]. \quad (51)$$

Because $\int_0^{2\pi} d\phi \ln(1 + \zeta^2 + 2\zeta \cos \phi) = 0$, the first term in square brackets vanishes. This was the only term that had a NNLL $\alpha_s^2 \ln M/p_t$ factor and so at NNLL accuracy $\mathcal{F}^{\text{clust}}$ is zero at large R , modulo $1/R$ corrections associated with the $1/R$ term in Eq. (47). The only element that survives the azimuthal integration in Eq. (51) is the second term in square brackets, resulting in

$$\mathcal{F}^{\text{clust}} = -8 \frac{\alpha_s^2 C^2}{\pi^2} R \zeta_3. \quad (52)$$

This is N³LL, so beyond our accuracy. Note, however, that it is enhanced by a factor of R . In the large R limit, the separation between partons is limited to be at most $2 \ln M/p_t$ and thus the R factor is effectively replaced with a coefficient of order $\ln M/p_t$. Consequently the apparently N³LL term of Eq. (52) is “promoted” and becomes a NNLL $\alpha_s^2 \ln M/p_t$ contribution. This is not accounted for in the purely NNLL R -dependent analysis that led to Eq. (46).

The exact infinite R result can be obtained at order $\alpha_s^2 L$ by evaluating $\mathcal{F}^{\text{clust}}$ with $J(k_1, k_2) = 1$, giving

$$\mathcal{F}^{\text{clust}} = 16 \frac{\alpha_s^2 C^2}{\pi^2} \int_0^1 \frac{d\zeta}{\zeta} \int_{-\pi}^{\pi} \frac{d\phi}{2\pi} \int_{p_t}^{\frac{p_t}{\sqrt{1+\zeta^2+2\zeta \cos \phi}}} \frac{dk_{t,1}}{k_{t,1}} \left(\ln \frac{M}{k_{t,1}} - \ln \zeta \right) \ln \frac{M}{k_{t,1}} = -4 \frac{\alpha_s^2}{\pi^2} \zeta_3 C^2 \ln \frac{M}{p_t} + \mathcal{O}(\alpha_s^2 \ln^0 \frac{M}{p_t}). \quad (53)$$

Note the agreement of the ζ_3 term here with that derived in Eq. (44). It is this contribution that corresponds to the ζ_3 term in Eq. (9).

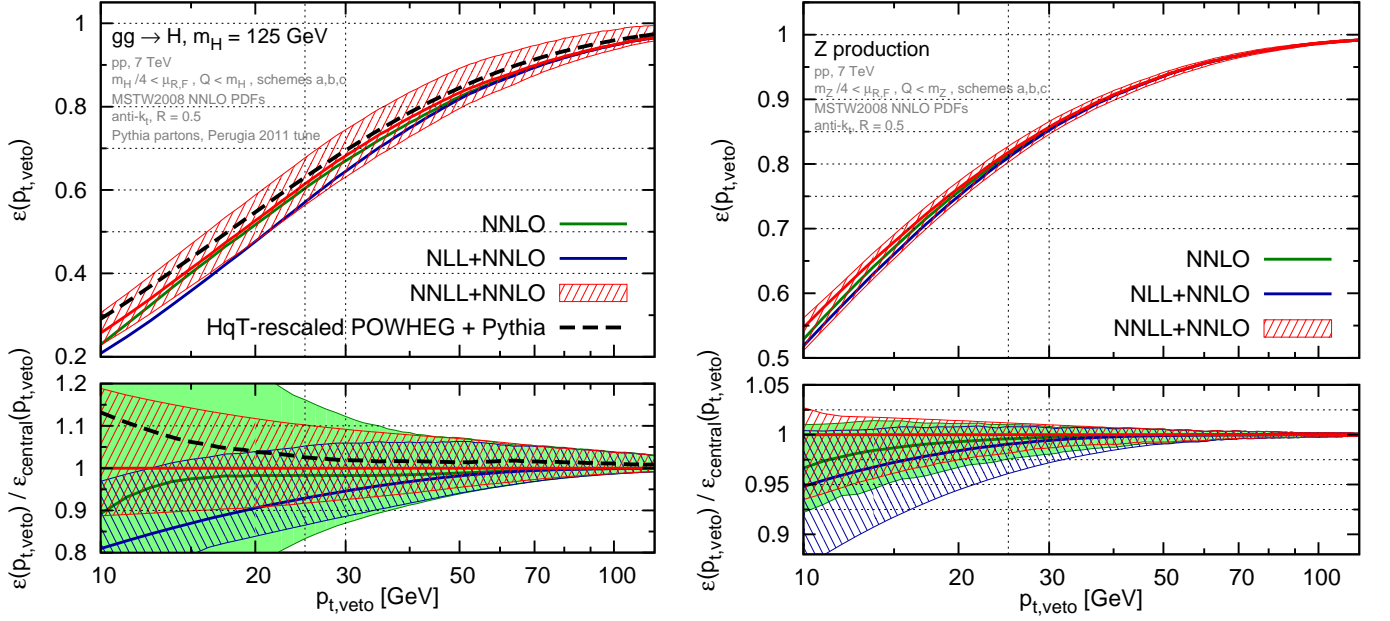


FIG. 3: Comparison of NNLO, NLL+NNLO and NNLL+NNLO results for the jet-veto efficiency for Higgs (left) and Z-boson (right) production at 7 TeV. The Higgs plot also includes the result from a POWHEG (revision 1683) [17, 37] plus Pythia (6.426) [14, 38] simulation in which the Higgs-boson p_t distribution has been reweighted to match the NNLL+NNLO prediction from HqT 2.0 [6] as in [18]. The lower panels show the results normalised to the central NNLL+NNLO curves.

4. Correlation matrix between 0-jet and inclusive 1-jet cross sections

As discussed in [18], the prescription that we propose for determining the uncertainties on the 0-jet cross section is to treat the uncertainties on the jet-veto efficiency and on the total cross section as uncorrelated. This gives the following covariance matrix for the uncertainties of the 0-jet ($\sigma_{0\text{-jet}}$) and inclusive 1-jet ($\sigma_{\geq 1\text{-jet}}$) cross sections:

$$\begin{pmatrix} \epsilon^2 \delta_\sigma^2 + \sigma^2 \delta_\epsilon^2 & \epsilon(1-\epsilon) \delta_\sigma^2 - \sigma^2 \delta_\epsilon^2 \\ \epsilon(1-\epsilon) \delta_\sigma^2 - \sigma^2 \delta_\epsilon^2 & (1-\epsilon)^2 \delta_\sigma^2 + \sigma^2 \delta_\epsilon^2 \end{pmatrix} \quad (54)$$

5. Results at 7 TeV

For completeness, we show in Fig. 3 results for 7 TeV centre of mass energy. The changes relative to the 8 TeV results are modest, with very slightly higher efficiencies at 7 TeV. This can be understood because at higher centre of mass energy, the PDFs are probed at lower x values, where the scale dependence is steeper, causing the efficiencies to drop off more rapidly as one decreases $p_{t,\text{veto}}$.

6. R dependence of results

Figure 4 shows the the jet veto efficiency as a function of $p_{t,\text{veto}}$ for several different jet-radius (R) values. Increasing the jet radius, more radiation is captured and therefore a jet is more likely to pass the $p_{t,\text{veto}}$ threshold and so be vetoed. Consequence the jet-veto efficiency is expected to be lower for larger R values. This is precisely as observed in Fig. 4.

Quantitatively, the differences between the $R = 0.4$ and $R = 0.5$ results (the values used respectively by ATLAS and CMS) are small compared to the uncertainties on the predictions. In contrast, for $R = 1$ the differences compared to the smaller- R results are not negligible. One interesting feature, commented on briefly in the main text, is that for the Higgs-boson case, the uncertainties are somewhat smaller for $R = 1$ than for $R = 0.4$ and $R = 0.5$, especially the upper part of the uncertainty band. This can be understood with the help of the observation that the upper edge of the uncertainty band for the small R values is set by the $Q = M_H$ variant of the resummation (recall that our default

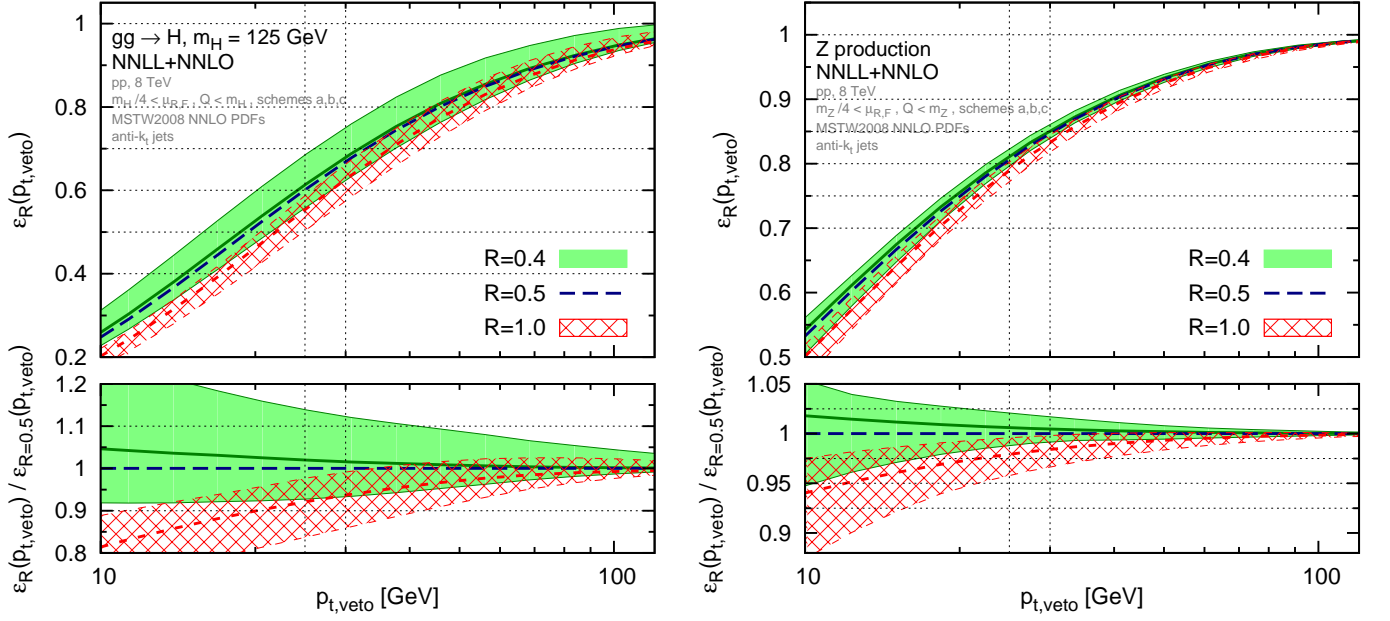


FIG. 4: Jet veto efficiency at NNLL+NNLO as a function of $p_{t,\text{veto}}$, comparing several jet-radius values; shown for pp collisions at a centre-of-mass energy of 8 TeV, for gluon-fusion Higgs production with $M_H = 125$ GeV (large m_{top} limit) and for Z -boson production. Uncertainty bands are shown only for $R = 0.4$ and $R = 1.0$ in order to enhance the clarity of the figure. The $R = 0.5$ uncertainty band is to be found in Fig. 2. The lower panels show the predictions normalised to the central $R = 0.5$ results.

Q is $M_H/2$). Using $Q = M_H$ increases the size of L . Since the $f^{\text{correl}}(R) + f^{\text{clust}}(R)$ function grows for small R and multiplies $\alpha_s^2 L$, a smaller R value magnifies the impact of an increase in Q .

If, experimentally, one were to consider using larger R values for performing jet vetoes in order to reduce the theoretical uncertainties, one concern might be the greater contamination of the jet's p_t from the underlying event and pileup. To some extent this could be mitigated by methods such as subtraction [61], filtering [62] or trimming [63]. Note that with subtraction and filtering (when the latter uses two filtering subjects, or more) our jet-veto predictions remain unchanged at NNLO and at NNLL accuracy.